



# HHS Public Access

Author manuscript

*Proteomics*. Author manuscript; available in PMC 2023 April 01.

Published in final edited form as:

*Proteomics*. 2022 April ; 22(7): e2100231. doi:10.1002/pmic.202100231.

## Quantitative proteomics revealed new functions of ALKBH4

Kailin Yu<sup>1</sup>, Tianyu F. Qi<sup>2</sup>, Weili Miao<sup>1</sup>, Xiaochuan Liu<sup>1</sup>, Yinsheng Wang<sup>1</sup>

<sup>1</sup>Department of Chemistry, University of California, Riverside, California, USA

<sup>2</sup>Environmental Toxicology Graduate Program, University of California, Riverside, California, USA

### Abstract

ALKBH4 is a versatile demethylase capable of catalyzing the demethylation of monomethylated lysine-84 on actin and *N*<sup>6</sup>-methyladenine in DNA. In this study, we conducted a quantitative proteomic experiment to reveal the altered expression of proteins in HEK293T cells upon genetic ablation of *ALKBH4*. Our results showed markedly diminished levels of *GSTP1* and *HSPB1* proteins in *ALKBH4*-depleted cells, which emanate from an augmented expression level of DNA (cytosine-5)-methyltransferase 1 (DNMT1) and the ensuing elevated cytosine methylation in the promoter regions of *GSTP1* and *HSPB1* genes. Together, our results revealed a role of ALKBH4 in modulating DNA cytosine methylation through regulating the expression level of DNMT1 protein.

### Keywords

bisulfite sequencing; cytosine methylation; mass spectrometry; parallel-reaction monitoring; post-translational modification; quantitative proteomics; SILAC

## 1 | INTRODUCTION

Fe(II)/2-oxoglutarate (2OG)-dependent dioxygenases catalyze the oxidative modifications of a diverse array of substrates that play important roles in various biological processes including collagen biosynthesis, hypoxia response, and epigenetic/epitranscriptomic regulation [1–3]. Among them, ALKBH family proteins, including ALKBH1–8 and FTO, are involved in repairing alkylation damage in DNA and demethylation of RNA [3, 4].

Within the ALKBH family proteins, ALKBH4 was found to assume diverse biological functions and be capable of demethylating monomethylated lysine or *N*<sup>6</sup>-methyl-2'-deoxyadenosine (6-mdA). ALKBH4 is essential during early development in mice and inducible knockout of *Alkbh4* gene in developing juvenile mice was shown to elicit defects in spermatogenesis [5, 6]. In addition, ALKBH4 modulates actin–myosin II interaction

**Correspondence:** Yinsheng Wang, Department of Chemistry, University of California, Riverside, CA 92521, USA. yinsheng@ucr.edu.

### CONFLICT OF INTEREST

The authors declare no conflict of interest.

### SUPPORTING INFORMATION

Additional supporting information may be found online <https://doi.org/10.1002/pmic.202100231> in the Supporting Information section at the end of the article.

through catalyzing the demethylation of mono-methylated lysine 84 (K84me1) on actin [5], which augments the interaction between actin and non-muscle myosin II, thereby modulating cytokinesis and cell migration. Furthermore, ALKBH4 regulates Polycomb silencing through demethylating 6-mda in DNA [7]. A yeast two-hybrid screening led to the identification of several ALKBH4-interacting proteins, which are associated with chromatin and/or involved with transcription, though global gene expression was only marginally changed upon overexpression of ALKBH4 [8].

We reason that a comprehensive assessment about how genetic depletion of ALKBH4 modulates protein expression at the global proteome scale may offer new insights into the biological functions of ALKBH4 protein. In the present study, we conducted such an analysis, and we found that CRISPR-mediated ablation of ALKBH4 led to substantial changes in expression of a large number of proteins, including the markedly diminished expression of GSTP1 and HSPB1 proteins. Mechanistically, these changes arise from elevated expression of DNMT1 and the ensuing epigenetic silencing of these two genes.

## 2 | MATERIALS AND METHODS

### 2.1 | CRISPR targeting of *ALKBH4* gene in HEK293T cells

CRISPR targeting of *ALKBH4* gene was conducted following previously described procedures except that a 20-bp single guide RNA (sgRNA) sequence targeting *ALKBH4* was used [9–11]. The successful knockout of *ALKBH4* gene was validated by Sanger sequencing and Western blot analysis (Figure S1).

### 2.2 | Cell culture

HEK293T and PC3 cells were cultured in DMEM media (Gibco) containing 10% fetal bovine serum (FBS), 2% L-glutamine, and 1% penicillin/streptomycin. The ALKBH4-deficient cells were cultured in DMEM media containing 10% FBS, 2% L-glutamine, 1% penicillin/streptomycin, and 1  $\mu$ g/mL puromycin. The cells were maintained at 37°C in a 5% CO<sub>2</sub> atmosphere.

### 2.3 | In-gel digestion of whole-cell lysates and LC-MS/MS analysis in the data-dependent acquisition (DDA) mode

One forward and two reverse SILAC (stable isotope labeling by amino acids in cell culture) experiments were conducted [12]. The lysates of heavy-labeled ALKBH4-knockout cells and light-labeled parental HEK293T cells were mixed at a 1:1 ratio (by mass, based on quantification using the Bradford assay) in the forward labeling experiment. The reverse labeling experiment was performed in the opposite way. The lysate mixtures were subsequently loaded onto a 10% SDS-PAGE gel and ran at 80 V for 2 h. The gel lanes were cut into 10 slices based on apparent molecular weights of proteins, and these gel slices were cut into ~1 mm<sup>3</sup> cubes. Proteins were digested in-gel, at 37°C overnight, with MS-grade trypsin (Pierce) at an enzyme/substrate ratio of 1:100 in 25 mM ammonium bicarbonate in H<sub>2</sub>O/CH<sub>3</sub>CN (9/1 v/v) [13]. After elution from the gel, the peptide fractions were dried in a Speed-vac and desalted with OMIX C18 Tips (Agilent Technologies). The samples were analyzed by LC-MS/MS in a DDA mode on a Q Exactive Plus hybrid

quadrupole-Orbitrap mass spectrometer (Thermo Scientific, CA) coupled with a Dionex UltiMate 3000 RSLCnano UPLC system. Maxquant, Version 1.5.2.834, was utilized to identify the light- and heavy-labeled peptides and quantify their intensity ratios, and UniProt database (UP000005640) was used for the database search.

#### 2.4 | Tryptic digestion and parallel-reaction monitoring (PRM)-based quantification of DNMT1 protein

The whole-cell protein lysates of HEK293T cells and the isogenic ALKBH4 knockout cells were denatured, reduced, alkylated, and digested with sequencing-grade trypsin following a previously published filter-aided sample preparation (FASP) protocol [14]. The resulting tryptic peptides were desalted using OMIX C18 pipette tips (Agilent Technologies). Stable isotope-labeled tryptic peptides of ALKBH4 (ELSAEFGPGG[<sup>13</sup>C<sub>6</sub>,<sup>15</sup>N<sub>4</sub>]R) and DNMT1 (FFLLENV[<sup>13</sup>C<sub>6</sub>,<sup>15</sup>N<sub>4</sub>]R) (New England Peptide, Inc.) were spiked into the tryptic digestion mixtures prior to LC-PRM analyses.

The LC-PRM experiments were carried out on the above-described Q Exactive Plus quadrupole-Orbitrap mass spectrometer coupled with a Dionex UltiMate 3000 RSLCnano UPLC system. Tryptic peptides (500 ng) spiked with 1.5 fmol stable isotope-labeled peptides of ALKBH4 and DNMT1 were loaded onto a 4 cm-long trapping column (150  $\mu$ m i.d.) packed with 5  $\mu$ m Reprosil-Pur C18-AQ resin (Dr. Maisch GmbH HPLC) and separated on a 25 cm-long analytical column (75  $\mu$ m i.d.) packed with 3  $\mu$ m Reprosil-Pur C18-AQ resin (Dr. Maisch GmbH HPLC). The flow rate was 300 nL/min, and a 125-min linear gradient of 6–43% acetonitrile in 0.1% formic acid was used. The PRM experiment was set up with a precursor ion isolation window of 1.0 *m/z*, an MS/MS resolution of 17,500, an automated gain control target of  $1 \times 10^5$ , and a normalized collision energy of 28.

MS/MS of peptides of ALKBH4 and DNMT1 were retrieved from shotgun proteomics data described elsewhere [15] and deposited into Skyline [16]. The raw LC-PRM files were imported into Skyline. Dot product (dotp) value [17] was calculated in Skyline for the evaluation of the similarity between the acquired MS/MS and the MS/MS deposited in the library. The relative abundances of ALKBH4 and DNMT1 were calculated from the ratio of the sum of the peak areas of fragment ions for the light-labeled peptides over their heavy-labeled counterparts.

#### 2.5 | Stable knockdown of ALKBH4 gene in HEK293T and PC3 cells

All primers and oligodeoxynucleotides used for the construction of shRNA plasmids were purchased from Integrated DNA Technologies. All shRNAs were cloned into the Age I/ EcoR I sites of the pLKO.1 vector (Addgene, plasmid #10878) with a puromycin resistance cassette. All constructs were confirmed by Sanger sequencing. Scrambled shRNA with a hairpin sequence of 5'-CCT AAG GTT AAG TCG CCC TCG CTC TAG CGA GGG CGA CTT AAC CTT AGG-3' (Addgene, Cambridge, MA, USA) was used as a negative control. Retrovirus was packaged in HEK293T cells by transfecting ALKBH4 shRNA-containing pLKO constructs together with two helper plasmids, that is, pCMV-dR8.2 and pCMV-VSV-G. Viral supernatants were harvested at 48 h following transfection and filtered before use. HEK293T and PC3 cells were subsequently infected with the harvested virus supernatants.

After 24 h, the cells were treated for 72 h with fresh complete medium containing 1.0 and 0.4  $\mu\text{g}/\text{mL}$  puromycin, respectively. The knockdown efficiencies were assessed by Western blot analysis.

## 2.6 | Transient overexpression of wild-type ALKBH4 and its catalytically inactive mutant (H169A/D171A)

The coding sequences of the wild-type and H169A/D171A mutant of *ALKBH4* gene were inserted into a pRK7 vector with a 3  $\times$  FLAG sequence at the 3'-terminus of the coding region of ALKBH4. The vectors were transiently transfected into ALKBH4 knockout cells with Transit-2020 reagent (Mirus). The cells were harvested at 48 h later for Western blot analysis.

## 2.7 | Western blot

The harvested cell pellets were washed with 1  $\times$  PBS buffer and lysed in the lysis buffer at 4°C for 30 min. The cell debris was removed by centrifugation and the protein concentrations were determined by Bradford assay (Bio-Rad). The protein lysates (30  $\mu\text{g}$ ) were resolved on a 10% SDS polyacrylamide gel (Bio-Rad). Proteins in the gel were transferred to a nitrocellulose membrane (Bio-Rad) and incubated with primary antibodies at 4°C overnight.

Rabbit polyclonal antibodies against ALKBH4 (ABclonal, A7812), DNMT1 (ABclonal, A5495), GSTP1 (ABclonal, A5691) and HSPB1 (ABclonal, A0240), and mouse polyclonal antibody against GAPDH (Santa Cruz Biotechnology, sc-47724) were employed as primary antibodies. Anti-rabbit IgG (whole molecule)-peroxidase antibody produced in goat (Sigma, #A0545) and m-IgG  $\kappa$  BP-HRP (Santa Cruz Biotechnology, sc-516102) were used as secondary antibodies.

## 2.8 | Real-time quantitative PCR (RT-qPCR)

Total RNA was extracted from HEK293T cells and the isogenic ALKBH4 knockout cells. The cDNA was subsequently produced by reverse transcription, purified using the QIAquick PCR purification Kit (Qiagen, MD) and used for RT-qPCR analysis. The primers used in RT-qPCR were: DNMT1 forward 5'-AGGGAAAAGGGAAGGGCAAG-3', DNMT1 reverse AGAAAACACATCCAGGGTCCG-3'; GAPDH forward 5'-TGCACCACCAACTGCTTAGC-3', GAPDH reverse 5'-GGCATGGACTGTGGTCATGAG-3'.

## 2.9 | Bisulfite sequencing

Approximately  $5 \times 10^3$  cells were collected, lysed, and treated with bisulfite using the EZ DNA Methylation-Direct Kit (Zymo Research, CA). The resulting DNA was subsequently amplified using ZymoTaq DNA Polymerase (Zymo Research, CA). Primers for *GSTP1* and *HSPB1* genes were designed using the MethPrimer 2.0 online tool (<http://www.urogene.org/methprimer2/>) to amplify 426- and 326-bp DNA fragments, respectively, of the promoter regions of the bisulfite converted genes. The outer PCR was set up using the following primers: GSTP1 forward primer, 5'-GGATYGTAGYGGTTTTAGGGAAT-3', GSTP1 reverse primer, 5'-CATACTAAAACTCTAAACCCCATC-3'; HSPB1

forward primer, 5'-GTTTAGGTTGGAGTGTAGTGG-3', HSPB1 reverse primer, 5'-AAAAAATTCAACCCTCATCTAAAAC-3'. The reaction mixture was heated to 95°C for 10 min followed by 36 cycles of denaturation at 95°C for 30 s, annealing at 55°C for 45 s, and elongation at 72°C for 1 min, followed by a final elongation step at 72°C for 7 min. The successful amplification and the size of the PCR amplicon were validated using electrophoresis on a 1.5% agarose gel. Amplicons were purified using the E.Z.N.A. Gel Extraction Kit (Omega Bio-tek, GA).

The purified PCR products were cloned into the pGEM-T vector (Promega Corporation, WI) and the ligation products were selected by blue/white colony screening. Ten white colonies selected for each cell line were grown in liquid Lysogeny broth (LB) media overnight, and the plasmids were extracted using GeneJET Plasmid Miniprep kit (Thermo Fisher Scientific, MA). The plasmids were then subjected to Sanger sequencing. Sequencing results were analyzed by the BiQ Analyzer software (<http://biq-analyzer.bioinf.mpi-inf.mpg.de/>) to generate the lollipop-representation. The methylation levels were subsequently determined.

### 3 | RESULTS

#### 3.1 | ALKBH4-deficient cells display diminished expression levels of GSTP1 and HSPB1 proteins

A major objective of the present study was to explore the biological functions of ALKBH4. To this end, we examined how genetic ablation of *ALKBH4* in HEK293T cells perturbs the global proteome. We employed SILAC [12], combined with SDS-PAGE fractionation and LC-MS/MS analysis in the DDA mode, to assess, at the proteome-wide scale, the differential expression of proteins in HEK293T cells after CRISPR-mediated ablation of *ALKBH4* gene (Figure S1).

By using this approach, we were able to quantify a total of 3177 proteins, among which 2090 were quantified from at least one cycle of forward and one cycle of reverse SILAC labeling experiments, and 1893 proteins were quantified in all three replicates of SILAC labeling experiments (Table S1). In comparison with the parental HEK293T cells, 104 and 47 proteins were substantially up- and downregulated (by at least 1.5-fold), respectively, in the ALKBH4-1 KO cells. Among the 47 downregulated proteins, GSTP1 and HSPB1 displayed marked decreases in ALKBH4 knockout background relative to parental HEK293T cells (Figure 1).

We confirmed the differential expressions of GSTP1 and HSPB1 by Western blot analysis (Figure 2). To exclude the possible off-target effect of sgRNA, we ectopically expressed wild-type ALKBH4 and its catalytically inactive mutant (i.e., H169A/D171A) in ALKBH4 knockout cells, and monitored the expression levels of these proteins by using Western blot analysis. Our results showed that wild-type ALKBH4, but not its catalytically inactive mutant, was able to restore the expression levels of GSTP1 and HSPB1 proteins in ALKBH4 knockout cells (Figure 2).

### 3.2 | The decreased expression levels of *GSTP1* and *HSPB1* in *ALKBH4*-deficient cells arise from their promoter hypermethylation

Previous studies showed that promoter hypermethylation results in epigenetic silencing of *GSTP1* and *HSPB1* genes [18]. To examine whether diminished expression of these two proteins in *ALKBH4*-deficient cells arises from a similar mechanism, we monitored the methylation status of CpG sites in the promoter region of *GSTP1* and *HSPB1* genes in *ALKBH4* KO and parental HEK293T cells by using bisulfite sequencing. Our results revealed that no methylation was detectable at any of the 47 CpG sites in the promoter region of *GSTP1* gene in parental HEK293T cells; the overall methylation levels, however, were 76.6% and 75.1% in the two clones of knockout cells, that is, *ALKBH4*-1 and *ALKBH4*-2 KO cells, respectively (Figure 3A–C). Likewise, the 16 CpG sites in the promoter region of *HSPB1* gene were entirely unmethylated in HEK293T cells, whereas the overall methylation levels at these sites were 69.4% in *ALKBH4*-1 KO and *ALKBH4*-2 KO cells, respectively (Figure 3D–F). These results demonstrate that the diminished expressions of *GSTP1* and *HSPB1* proteins in *ALKBH4* KO cells emanate from epigenetic silencing of these two genes through elevated methylation at CpG sites in their promoters.

### 3.3 | Differential expression of *DNMT1* in HEK293T and the isogenic *ALKBH4*-deficient cells

Considering the roles of *DNMT1* in DNA methylation in gene promoters, we next investigated the expression levels of *DNMT1* in HEK293T cells and the isogenic *ALKBH4*-deficient cells. We applied a PRM-based targeted quantitative proteomic method to quantify tryptic peptides derived from *DNMT1* and *ALKBH4* in the aforementioned *ALKBH4* knockout cells and parental HEK293T cells. Stable isotope-labeled peptides of *ALKBH4* (ELSAEFGPGG[<sup>13</sup>C<sub>6</sub>, <sup>15</sup>N<sub>4</sub>]R) and *DNMT1* (FFLLENV[<sup>13</sup>C<sub>6</sub>, <sup>15</sup>N<sub>4</sub>]R) were utilized as internal standards to quantify these two proteins. We manually examined the co-elution of four to six fragment ions from the same precursor ions, the co-elution of the endogenous peptide and the internal standard, and used dot product (dotp) larger than 0.7 for positive identification. We then examined the relative levels of *ALKBH4* and *DNMT1* proteins in *ALKBH4* knockout cells over parental HEK293T cells. Our results showed that, as expected, the *ALKBH4* protein was nearly undetectable in the knockout background (Figure S2). On the other hand, *DNMT1* protein exhibits 1.7- and 1.9-fold increases in *ALKBH4*-1 KO and *ALKBH4*-2 KO cells, respectively (Figure 4A, B). This is consistent with the results obtained from Western blot analysis (Figure 2). Moreover, we found that the mRNA levels of *DNMT1* display an ~2-fold increase in the two lines of *ALKBH4* KO cells relative to parental 293T cells, suggesting that the increase in *DNMT1* protein in the KO cells arises from transcriptional upregulation (Figure 4C).

### 3.4 | Overexpression of *ALKBH4* can partly rescue *DNMT1* protein level in *ALKBH4*-deficient cells

To further substantiate the role of *ALKBH4* in modulating the expression level of *DNMT1*, we complemented the *ALKBH4* knockout cells with ectopic expression of wild-type *ALKBH4* and its catalytically inactive mutant, where two amino acids that are crucial in Fe(II) binding were both mutated to alanine (i.e., the H169A/D171A mutant), and examined

the expression level of DNMT1 protein by Western blot analysis. Our results revealed that reconstitution with the wild-type ALKBH4 restored the DNMT1 protein to a level that is close to parental HEK293T cells; the mutant ALKBH4, however, failed to do so (Figure 2). These results further supported that ALKBH4 negatively modulates the expression level of DNMT1 protein, and this regulation entails the catalytic activities of ALKBH4.

### 3.5 | shRNA-mediated stable knockdown of ALKBH4 in HEK293T and PC3 cells led to elevated expression of DNMT1 and decreased expression of GSTP1 and HSPB1

A potential limitation of the above results resides in that the CRISPR targeting was conducted using a single sgRNA (Figure S1), which may elicit off-target effects. To address this and to further verify the ALKBH4-mediated regulation of DNMT1, we employed shRNA to stably knockdown the expression of *ALKBH4* gene in HEK293T cells with three different sequences of shRNAs. For comparison, we also generated HEK293T cells with stable expression of a control shRNA (shCtrl). Our results from Western blot analysis revealed that the shRNA-mediated knockdown of ALKBH4 resulted in increased expression levels of DNMT1 by 1.7- and 1.9-fold, which is accompanied with attenuated expression levels of GSTP1 and HSPB1 (Figure 5A, B). This is consistent with the observations made in HEK293T cells where the *ALKBH4* gene was ablated by CRISPR-Cas9.

An earlier study showed that *GSTP1* gene is expressed in PC3 prostate cancer cells and this gene exhibits both methylated and unmethylated GSTP1 alleles [18]. To explore whether this ALKBH4-DNMT1 pathway is general, we generated PC cells with the *ALKBH4* gene being stably knockdown using three separate sequences of shRNA (Figure 5C, D). Our Western blot results showed that stable knockdown of *ALKBH4* gene again led to elevated level of DNMT1 protein and diminished levels of GSTP1 and HSPB1 proteins in PC3 cells (Figure 5C, D).

## 4 | DISCUSSION

Previous studies revealed ALKBH4 as a versatile enzyme involved in demethylation of K84me1 in actin and 6-mdA in DNA [5, 7]. Loss of ALKBH4 was found to elicit defects in cytokinesis in cultured cells and spermatogenesis in developing juvenile mice [5, 6]. ALKBH4 was also shown to interact with chromatin-associated proteins and/or proteins involved in transcription [8]. However, it has not been examined how genetic depletion of ALKBH4 perturbs the human proteome. By employing an SILAC-based quantitative proteomic workflow, we demonstrated that CRISPR-mediated ablation of ALKBH4 led to alterations in expression levels of a large number of proteins, including the pronouncedly attenuated expression of HSPB1 and GSTP1. Mechanistic studies revealed that loss of ALKBH4 led to elevated expression of DNMT1 protein, which result in augmented promoter methylation and the ensuing epigenetic silencing of *HSPB1* and *GSTP1* genes.

In light of the recent report that ALKBH4 catalyzes the demethylation of 6-mdA in DNA [7], our study provides a plausible crosstalk between the two types of methylation in DNA, that is, 6-mdA and 5-mdC, where ALKBH4 may not only lead to demethylation of 6-mdA, but also diminish the level of 5-mdC through negatively regulating the expression level of DNMT1, a maintenance DNA (cytosine-5)-methyltransferase that is required for

maintaining cytosine methylation during cell division. However, the molecular mechanism through which ALKBH4 depletion results in increased DNMT1 expression is unclear and awaits further investigation.

## Supplementary Material

Refer to Web version on PubMed Central for supplementary material.

## ACKNOWLEDGMENT

This work was supported by the National Institutes of Health (R35 ES031707).

### Funding information

National Institutes of Health, Grant/Award Number: R35 ES031707

## DATA AVAILABILITY STATEMENT

All the LC-MS/MS raw files and MaxQuant searching files were deposited to the ProteomeXchange Consortium via the PRIDE [19] partner repository with the dataset identifier PXD028148.

## REFERENCES

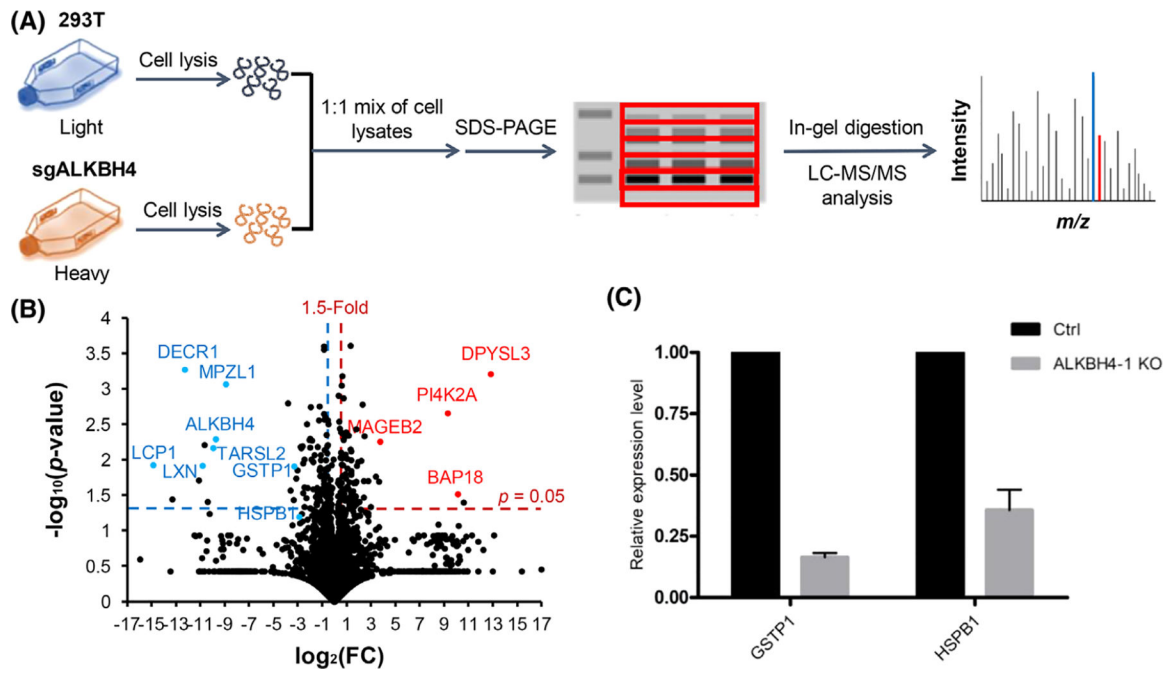
- Herr CQ, & Hausinger RP (2018). Amazing diversity in biochemical roles of Fe(II)/2-oxoglutarate oxygenases. *Trends in Biochemical Sciences*, 43, 517–532. [PubMed: 29709390]
- Islam MS, Leissing TM, Chowdhury R, Hopkinson RJ, & Schofield CJ (2018). 2-Oxoglutarate-dependent oxygenases. *Annual Review of Biochemistry*, 87, 585–620.
- Xu G-L, & Bochtler M (2020). Reversal of nucleobase methylation by dioxygenases. *Nature Chemical Biology*, 16, 1160–1169. [PubMed: 33067602]
- Shen L, Song C-X, He C, & Zhang Y (2014). Mechanism and function of oxidative reversal of DNA and RNA methylation. *Annual Review of Biochemistry*, 83, 585–614.
- Li M-M, Nilsen A, Shi Y, Fusser M, Ding Y-H, Fu Y, Liu B, Niu Y, Wu Y-S, Huang C-M, Olofsson M, Jin K-X, Lv Y, Xu X-Z, He C, Dong M-Q, Rendtlew Danielsen JM, Klungland A, & Yang Y-G (2013). ALKBH4-dependent demethylation of actin regulates actomyosin dynamics. *Nature Communications*, 4, 1832.
- Nilsen A, Fusser M, Greggains G, Fedorcsak P, & Klungland A (2014). ALKBH4 depletion in mice leads to spermatogenic defects. *PLoS One*, 9, e105113. [PubMed: 25153837]
- Kweon S-M, Chen Y, Moon E, Kvederaviciut K, Klimasauskas S, & Feldman DE (2019). An adversarial DNA  $N^6$ -methyladenine-sensor network preserves polycomb silencing. *Molecular Cell*, 74, 1138–1147.e6. [PubMed: 30982744]
- Bjørnstad LG, Meza TJ, Otterlei M, Olafsrud SM, Meza-Zepeda LA, & Falnes PØ (2012). Human ALKBH4 interacts with proteins associated with transcription. *PLoS One*, 7, e49045. [PubMed: 23145062]
- Doench JG, Fusi N, Sullender M, Hegde M, Vaimberg EW, Donovan KF, Smith I, Tothova Z, Wilen C, Orchard R, Virgin HW, Listgarten J, & Root DE (2016). Optimized sgRNA design to maximize activity and minimize off-target effects of CRISPR-Cas9. *Nature Biotechnology*, 34, 184–191.
- Sanson KR, Hanna RE, Hegde M, Donovan KF, Strand C, Sullender ME, Vaimberg EW, Goodale A, Root DE, Piccioni F, & Doench JG (2018). Optimized libraries for CRISPR-Cas9 genetic screens with multiple modalities. *Nature Communications*, 9, 5416.
- Wu J, Li L, Wang P, You C, Williams NL, & Wang Y (2016). Translesion synthesis of  $O^6$ -alkylthymidine lesions in human cells. *Nucleic Acids Research*, 44, 9256–9265. [PubMed: 27466394]



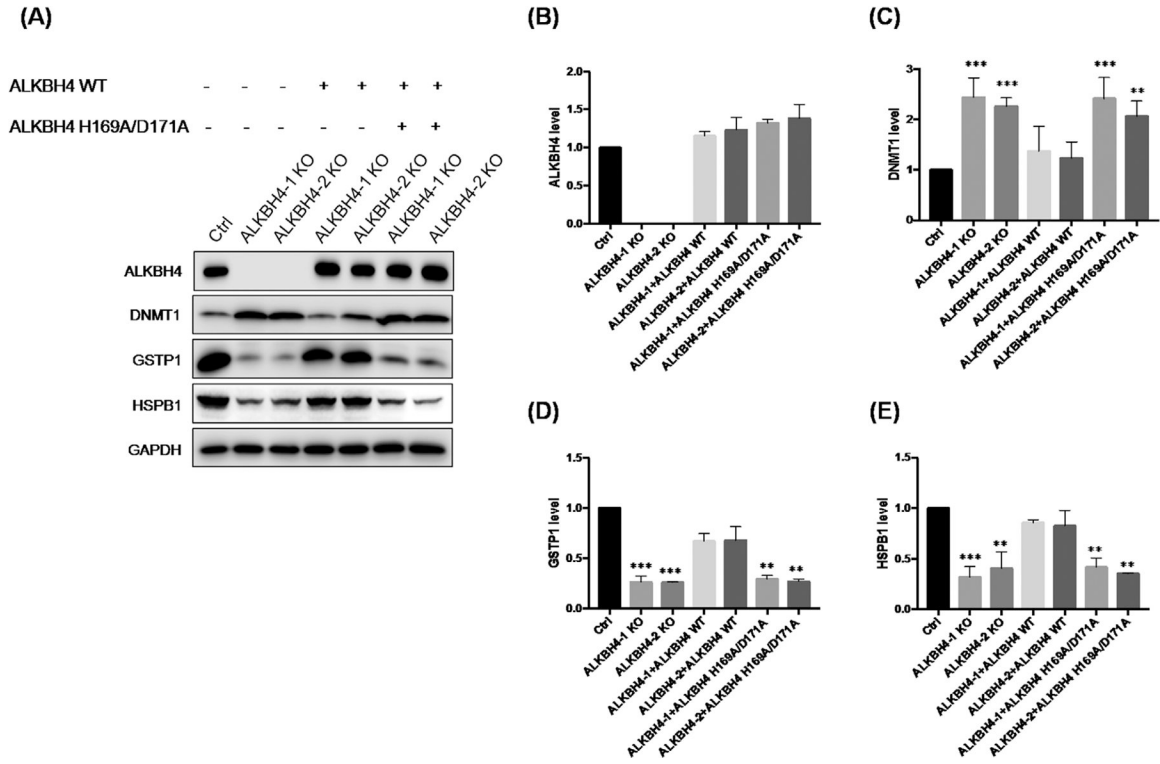
12. Ong S-E, Blagoev B, Kratchmarova I, Kristensen DB, Steen H, Pandey A, & Mann M (2002). Stable isotope labeling by amino acids in cell culture, SILAC, as a simple and accurate approach to expression proteomics. *Molecular and Cellular Proteomics*, 1, 376–386. [PubMed: 12118079]
13. Shevchenko A, Tomas H, Havli J, Olsen JV, & Mann M (2006). In-gel digestion for mass spectrometric characterization of proteins and proteomes. *Nature Protocols*, 1, 2856–2860. [PubMed: 17406544]
14. Wi niewski JR, Zougman A, Nagaraj N, & Mann M (2009). Universal sample preparation method for proteome analysis. *Nature Methods*, 6, 359–362. [PubMed: 19377485]
15. Miao W, Li L, & Wang Y (2018). A targeted proteomic approach for heat shock proteins reveals DNAJB4 as a suppressor for melanoma metastasis. *Analytical Chemistry*, 90, 6835–6842. [PubMed: 29722524]
16. Maclean B, Tomazela DM, Shulman N, Chambers M, Finney GL, Frewen B, Kern R, Tabb DL, Liebler DC, & Maccoss MJ (2010). Skyline: An open source document editor for creating and analyzing targeted proteomics experiments. *Bioinformatics*, 26, 966–968. [PubMed: 20147306]
17. Sherwood CA, Eastham A, Lee LW, Risler J, Vitek O, & Martin DB (2009). Correlation between y-type ions observed in ion trap and triple quadrupole mass spectrometers. *Journal of Proteome Research*, 8, 4243–4251. [PubMed: 19603825]
18. Singal R, van Wert J, & Bashambu M (2001). Cytosine methylation represses glutathione S-transferase P1 (GSTP1) gene expression in human prostate cancer cells. *Cancer Research*, 61, 4820–4826. [PubMed: 11406558]
19. Perez-Riverol Y, Csordas A, Bai J, Bernal-Llinares M, Hewapathirana S, Kundu DJ, Inuganti A, Griss J, Mayer G, Eisenacher M, Pérez E, Uszkoreit J, Pfeuffer J, Sachsenberg T, Yılmaz , Tiwary S, Cox J, Audain E, Walzer M, ... Vizcaíno JA (2019). The PRIDE database and related tools and resources in 2019: Improving support for quantification data. *Nucleic Acids Research*, 47, D442–D450. [PubMed: 30395289]

### Significance Statement

ALKBH4 is known to catalyze the demethylation of lysine-84 on actin and  $N^6$ -methyladenine in DNA. We performed a quantitative proteomic experiment to examine the differences in protein expression in HEK293T cells upon genetic ablation of *ALKBH4*. Our results demonstrated attenuated expression of GSTP1 and HSPB1 proteins in ALKBH4-depleted cells, which arises from an elevated expression level of DNA (cytosine-5)-methyltransferase 1 (DNMT1) and the ensuing elevated cytosine methylation in the promoter regions of *GSTP1* and *HSPB1* genes. Together, our results revealed a role of ALKBH4 in modulating DNA cytosine methylation through regulating the expression level of DNMT1 protein. Thus, this study represents the application of state-of-the-art proteomic approach for revealing new biological functions of ALKBH4.

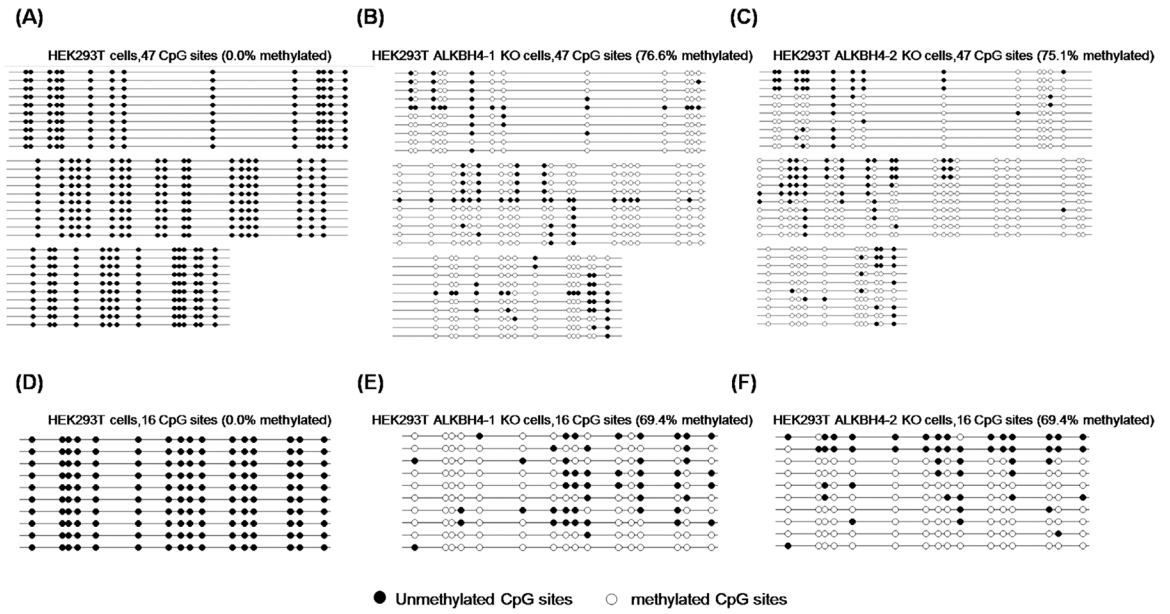
**FIGURE 1.**

DDA analyses for evaluating the differential expression of proteins in the whole cell lysates in HEK293T cells and the isogenic ALKBH4-deficient cells. (A) A schematic diagram showing the forward SILAC-based shotgun proteomic workflow for assessing the differences in protein expression in HEK293T cells and the isogenic ALKBH4 KO cells. (B) Volcano plot showing the quantification results of relative protein expression levels in HEK293T and the isogenic ALKBH4 KO cells in forward and reverse SILAC labeling experiments. Vertical dashed lines indicate a 1.5-fold increase (red) or decrease (blue) in expression in ALKBH4 KO over parental cells, and the horizontal dashed line denotes a  $p$  value of 0.05. (C) The quantification data of GSTP1 and HSPB1 proteins obtained from DDA analyses. The data represented the mean  $\pm$  SD ( $n = 3$ ). The  $p$  values were calculated based on unpaired, two-tailed Student's  $t$ -test: \*0.01  $p < 0.05$ ; \*\*0.001  $p < 0.01$ ; \*\*\* $p < 0.001$ . DDA, data-dependent acquisition; SD, standard deviation



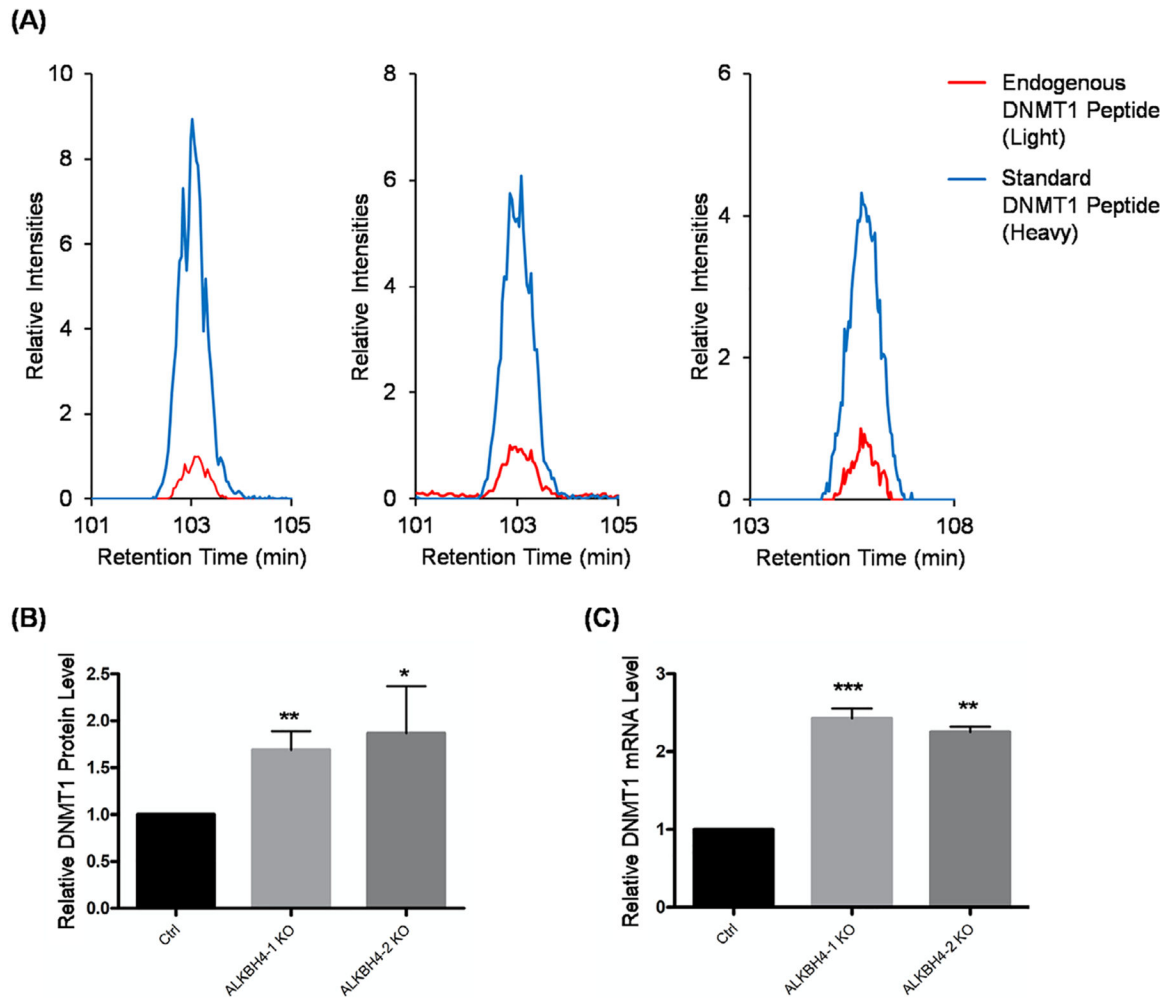
**FIGURE 2.**

Genetic ablation of ALKBH4 led to increased DNMT1 protein level and diminished levels of GSTP1 and HSPB1 proteins, which could be rescued by ectopic-overexpression of ALKBH4, but not its catalytically inactive mutant. (A) Western blot analysis confirmed the expression level change of DNMT1, GSTP1, and HSPB1 in ALKBH4-deficient cells. At 48 h, after transfection of ALKBH4 and ALKBH4 H169A/D171A into ALKBH4-deficient cells, the cells were harvested and lysates were used to monitor the levels of DNMT1, GSTP1, and HSPB1 proteins by Western blot analysis. (B–F) The changes in protein expression levels were quantified from band intensities using Image J. The intensities of the target proteins were divided by the corresponding band intensities of GAPDH, and the resulting ratios were further normalized against those observed in parental HEK293T cells. The data were presented as mean  $\pm$  SD (n = 3). The *p* values were calculated based on unpaired, two-tailed Student's *t*-test: \*\*0.001  $p$  < 0.01; \*\*\* $p$  < 0.001. SD, standard deviation



**FIGURE 3.**

Promoter methylation status of *GSTP1* and *HSPB1* genes in parental HEK293T cells and ALKBH4-deficient cells. Bisulfite sequencing demonstrated the methylation status of CpG sites in the promoter region of *GSTP1* (A–C) and *HSPB1* genes (D–F) in HEK293T cells and ALKBH4 KO cells. Higher levels of methylation were observed in the ALKBH4 KO cells than HEK293T cells. Each horizontal line represents one separate clone sequenced; filled and open circles designate unmethylated and methylated CpG sites, respectively

**FIGURE 4.**

LC-PRM for assessing the differential expression of DNMT1 protein in parental HEK293T cells and the isogenic ALKBH4-deficient cells. (A) Representative PRM traces for a tryptic peptide derived from DNMT1 protein. (B) The quantification data obtained from the PRM analyses. (C) The mRNA expression level of *DNMT1* gene in ALKBH4-deficient cells is displayed relative to the level observed in parental HEK293T cells. The values were normalized against the mRNA level of *GAPDH* gene. The data in (B) and (C) were presented as mean  $\pm$  SD (n = 3). The *p* values were calculated based on unpaired, two-tailed Student's *t*-test: \*0.01  $p < 0.05$ ; \*\*0.001  $p < 0.01$ ; \*\*\* $p < 0.001$ . PRM, parallel-reaction monitoring; SD, standard deviation

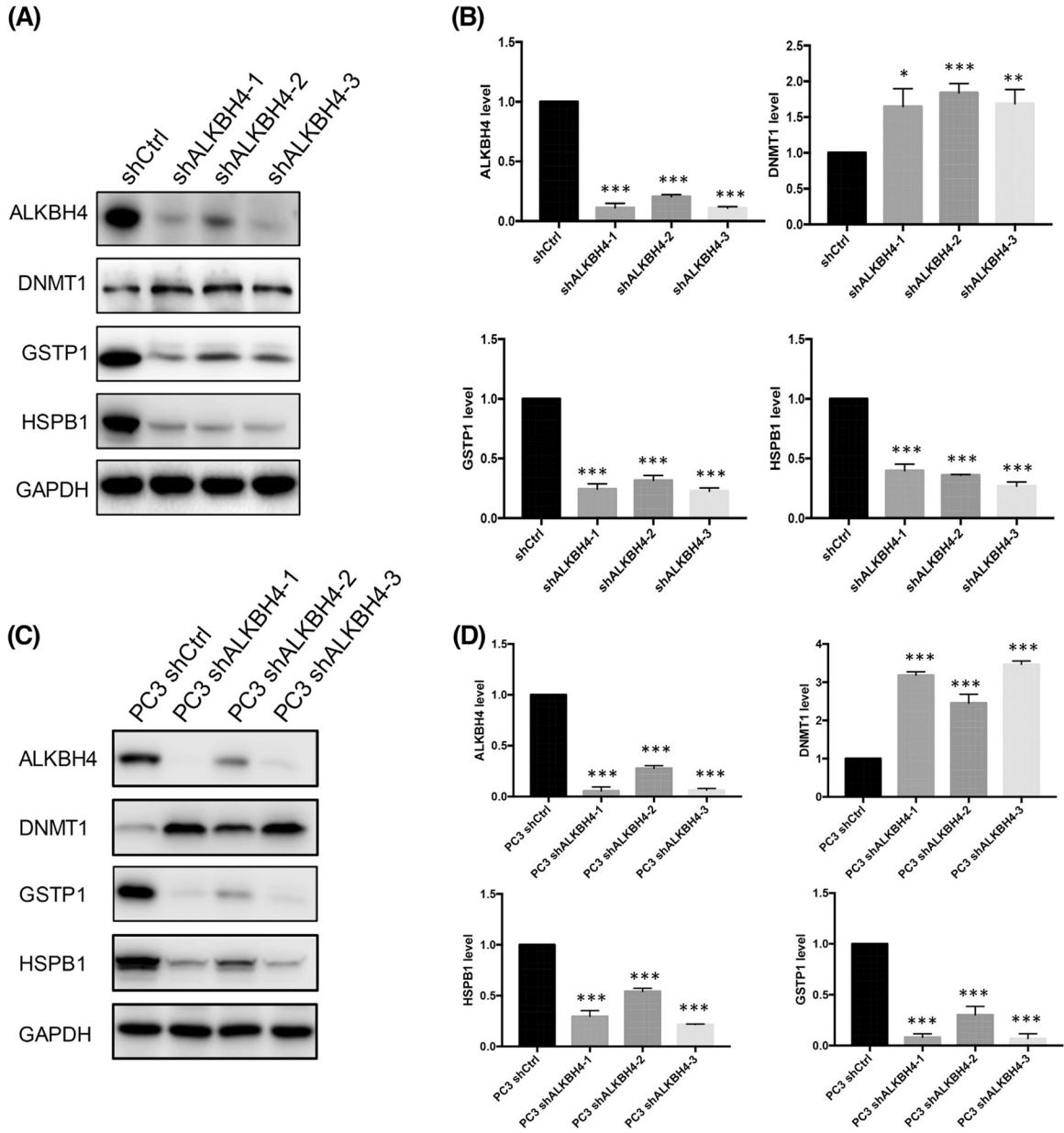


**FIGURE 5.**

shRNA-mediated knockdown of *ALKBH4* results in increased level of DNMT1 protein and diminished expression levels of GSTP1 and HSPB1 proteins in HEK293T cells and PC3 cells. (A) Western blot analysis showing the altered expression levels of DNMT1, GSTP1, and HSPB1 proteins in *ALKBH4*-knockdown relative to parental HEK293T cells. (B) The changes in expression levels of target proteins in HEK293T cells and the corresponding *ALKBH4* knockdown cells. (C) Western blot images for monitoring the expression levels of DNMT1, GSTP1, HSPB1, and GAPDH proteins in PC3 cells after shRNA-mediated knockdown of *ALKBH4* gene. (D) Quantification results for the changes in expression levels of DNMT1, GSTP1, and HSPB1 proteins in PC3 cells upon shRNA-mediated knockdown of *ALKBH4* gene. The band intensities for the target proteins were

quantified using Image J and divided by that of GAPDH, and the resulting ratios were normalized against the corresponding ratios measured for the PC3 cells treated with control non-targeting shRNA. The data in (B) and (D) were presented as mean  $\pm$  SD (n = 3). The *p* values were calculated based on unpaired, two-tailed Student's *t*-test: \*0.01  $p < 0.05$ ; \*\*0.001  $p < 0.01$ ; \*\*\* $p < 0.001$ . SD, standard deviation